

**Clustering of loose groups and galaxies
from the Perseus–Pisces Survey**

Roberto Trasarti Battistoni¹, Gianluca Invernizzi², & Silvio A. Bonometto³

Dipartimento di Fisica dell'Università, Via Celoria 16, 20133 Milano, Italy

Received _____; accepted _____

Submitted to ApJ, May 1996, astro-ph/9606116

arXiv:astro-ph/9606116v1 19 Jun 1996

¹e-mail: trasarti@astmiu.uni.mi.astro.it

²e-mail: laurbonom@astmiu.uni.mi.astro.it.

³e-mail: bonometto@mi.infn.it.

ABSTRACT

We investigate the clustering properties of loose groups in the Perseus–Pisces redshift Survey. Previous analyses based on CfA and SSRS surveys led to apparently contradictory results. We investigate the source of such discrepancies, finding satisfactory explanations for them. Furthermore, we find a definite signal of group clustering, whose amplitude A_G exceeds the amplitude A_g of galaxy clustering ($A_G = 14.5_{-3.0}^{+3.8}$, $A_g = 7.42_{-0.19}^{+0.20}$ for the most significant case; distances are measured in $h^{-1}\text{Mpc}$). Groups are identified with the adaptive Friends–Of–Friends (FOF) algorithms HG (Huchra & Geller 1982) and NW (Nolthenius & White 1987), systematically varying all search parameters. Correlation strength is especially sensitive to the sky–link D_L (increasing for stricter normalization D_0), and to the (depth m_{lim} of the) galaxy data. It is only moderately dependent on the galaxy luminosity function $\phi(L)$, while it is almost insensitive to the redshift–link V_L (both to the normalization V_0 and to the scaling recipes HG or NW).

Subject headings: cosmology: Large Scale Structure of the Universe
– galaxies: clustering

1. Introduction

Galaxy, group and cluster distributions probe matter clustering in the Universe, not only over different scales, but also for different density contrasts. However, while galaxy and cluster clustering have been widely inspected, a measurement of group clustering meets several conceptual and technical difficulties and it is not surprising that its results are controversial and partially contradictory.

In this note we report the result of an analysis of clustering properties of loose groups in the Perseus–Pisces redshift Survey (hereafter PPS; see Giovanelli, Haynes, & Chincarini 1986; Haynes et al. 1988; Giovanelli & Haynes 1989, 1991, 1993). Through such analysis we believe that the reasons of previous discrepant results become clear. It is also worth soon mentioning that our error analysis, based on bootstrap criteria, detects a precise signal of clustering for loose groups above statistical noise.

As is known, the 2–point functions of galaxies and clusters are consistent with the power laws

$$\xi_{gg} = A_g r^{-\gamma} , \quad \xi_{cc} = A_c r^{-\gamma} , \quad (1)$$

characterized by the same exponent $\gamma \simeq 1.8$, but by widely different amplitudes A_g and A_c . The detection of such difference (Bahcall & Soneira 1983, Klypin & Kopylov 1983) led Kaiser (1984) and Politzer & Wise (1984) to suggest the mechanism of biased galaxy formation.

Results are far less clear for galaxy groups. Jing & Zhang (1988, hereafter JZ88) and Maia & daCosta (1990, hereafter MdC90) claimed that the 2–point function for groups is still consistent with a power law $\xi_{GG}(r) = A_G r^{-\tilde{\gamma}}$ with $\tilde{\gamma} = 1.8$ and $A_G = A_g/d$ with $d \simeq 2\text{--}2.5$. On the contrary, Ramella, Geller, & Huchra (1990, hereafter RGH90) found $\xi_{GG}(r) \simeq \xi_{gg}(r)$ and, although their analysis cannot reject a value $\tilde{\gamma} = 1.8$, the preferred

value ranges around 1. According to RGH90, the main contribution to ξ_{GG} comes from the 2-point function ξ_{mm} of galaxies members of groups.

Recently Frederic (1995a&b, hereafter F95) determined $\xi(r)$ for haloes and halo groups in CDM simulations by Gelb (1992). He found groups to be significantly more correlated than single halos, and interpreted this as contrasting with RGH90’s results for galaxies and galaxy groups (but he also showed that the correlation strength depends on the prescription adopted for halo identification and illumination).

In all the above mentioned studies, groups were identified with the adaptive Friends-Of-Friends algorithms of Huchra & Geller (1982; HG82 hereafter) or Nolthenius & White (1987; hereafter NW87). Such algorithms require several input parameters. Some (the galaxy luminosity function $\phi(L)$ and the magnitude limit m_{lim}) are set by the data themselves. Others (the “sky-link” D_0 and the “redshift-link” V_0) must be decided by the user: D_0 can be related to the normalization ϕ_* of $\phi(L)$ (NW87), while the choice of V_0 is more complex (HG82; NW87; Ramella, Geller, & Huchra 1989, RGH89 hereafter). As already pointed out by NW87, confirmed by RGH89, and stressed by Nolthenius, Klypin, & Primack (1994, 1995; hereafter NKP94&95), a delicate point in group analysis is the *sensitivity* of the results to the details of the adopted algorithm and/or data set. Also forgetting possible intrinsic differences among the galaxy samples where groups were drawn from, the different search parameters of the algorithm used to identify galaxy groups could be at the origin of the above mentioned discrepancies. However, as we shall see below, this is actually more relevant for internal than for clustering properties (F95; Trasarti Battistoni 1995, 1996 – TB96 hereafter). Another problem is the high noise in the determination of ξ_{GG} , due to the limited extension of the group catalogs previously studied.

Loose groups in PPS were systematically identified and analyzed in TB96, who concentrated mainly on internal properties and their dependence on the adopted algorithm

and/or data sample. Differences between data samples are small but detectable, and the effect of the magnitude limit m_{lim} is to be properly taken into account. Note that PPS is wider than the CfA2 Slices (de Lapparent, Geller, & Huchra 1986, 1988, 1989 – dLGH86/88/89 hereafter; Geller & Huchra 1989; Huchra et al. 1990, Huchra, Geller, & Corwin 1995) used by RGH89–90 and F95, and is spatially disconnected from them as it lies in a different galactic hemisphere. It is also deeper than the redshift surveys CfA1 (Davis & Huchra 1982, Davis et al. 1982, Huchra et al. 1983) and SSRS1 (da Costa et al. 1988), where groups identified by Geller & Huchra (1983; hereafter GH83) and Maia, daCosta, & Latham (1989; hereafter MdCL89) were used by JZ88 and MdC90, respectively. In fact, the number of groups in PPS is ~ 180 -200, while it is $\lesssim 100$ -150 in the other samples, and this helps to reduce the above mentioned statistical noise.

Internal properties of groups have been used to constrain cosmological models and, in particular, the dark matter composition (NKP94&95). Also group clustering has been suggested as a test for cosmological models, both on analytical bases (e.g., Kashlinsky 1987), or through the comparison with numerical N–body simulations (F95). In the latter case, the key point is that galaxy groups can be identified automatically and *exactly in the same way* both from galaxy catalogs and from large ($R \simeq 100 h^{-1}\text{Mpc}$) N–body simulations (NW87; Moore, Frenk, & White 1993; NKP94&95; F95). Although such groups are basically expected to be physical objects this is no longer the basic requirement to have an effective comparison. Once groups are suitably defined, then properties are compared to find out which simulation best matches the observations.

There is a precise physical reason which favours loose groups over single galaxies (and compact groups) or rich clusters as a test of cosmological models. At intermediate separations ($\simeq 10 h^{-1}\text{Mpc}$), mass scales ($M \simeq 10^{13}M_{\odot}$), and density contrast ($\delta n/n \gtrsim 10$ –100) typical of galaxy groups, gravitational evolution is still in the mildly non–linear regime.

Therefore, LSS keeps memory of the shape of the post-recombination power spectrum $P(k)$. At larger scales linearity keeps the LSS signal at a level too low in respect to the noise, so $P(k)$ is not easily detectable, and the limited extension (in volume and number of objects) of available observational samples is often a problem. At smaller scales stronger non-linear and non-gravitational effects complicate everything.

Moreover, the most widely studied observational samples of rich clusters (Abell 1958; Abell, Corwin, Olowin 1989) suffer of various biases (Sutherland 1988; see Borgani 1995 for a review), mainly due to partially subjective criteria used in their compilation. Compact groups and rich clusters were recently identified from observational samples also employing objective and automatic procedures (Prandoni, Iovino, & MacGillivray 1994; Nichol et al. 1992; Dalton et al. 1992; Nichol, Briel, & Henry 1994). However such procedures are difficult to reproduce on N-body simulations. This is due to a combined need of high resolution (to ease object identification), large sample volume (to have a statistically meaningful number of objects), and computational speed (to reach a statistically meaningful number of independent realizations of the same theoretical model). In the case of clusters, the latter two difficulties can be circumvented by using a combination of numerical and analytical approaches based on the Zel'dovich approximation (e.g., Sahni & Coles 1995; Borgani et al. 1995), but the identification of observational-like clusters is still not an easy task.

The plan of the paper is the following. In Section 2 we describe the galaxy data and the group catalogs, while Section 3 describes the estimation of clustering properties. Results are presented and discussed in Section 4. We summarize our conclusions in Section 5.

2. Galaxy Data and Group Catalogs

The PPS database was compiled by Giovanelli & Haynes in the last decade (see Giovanelli & Haynes 1991, 1993; Wegner, Giovanelli, & Haynes 1993, and the references therein). The full redshift survey is magnitude-limited down to $m_Z \leq 15.7$, and now it covers the whole region $-2^h.00 \leq \alpha \leq +4^h.00$ and $0^\circ \leq \delta \leq 50^\circ$. As in TB96, we restricted to the region $-1^h.50 \leq \alpha \leq +3^h.00$ and $0^\circ \leq \delta \leq 40^\circ$, to avoid regions of high interstellar extinction. Magnitudes are anyway corrected as in Burstein & Heiles (1978), and redshifts are corrected for galactic rotation and Local Group motion as in Yahil, Sandage, & Tamman (1977). The two subsamples PPS1 and PPS2 (shown in Fig. 1, top panels) are magnitude-limited to $m_Z \leq 14.5$ and 15.5 respectively, in analogy with CfA1 and CfA2. This makes our comparison of data sample as clean as possible. In fact, the selection criteria of SSRS makes it qualitatively different from CfA or PPS. On the other hand, the full CfA1 (North+South) and the first two CfA2 Slices in the North are neither fully disjoint (as PPS2 and CfA2 Slices) nor one a subset of the other (as PPS1 of PPS2). The shape of the survey is also important. It is more difficult to identify groups in the proximity of the edges, so wide angle surveys are favoured over thin slices or pencil beams. To summarize, PPS1 (PPS2) covers a solid angle $\omega = 0.76 \text{ sr}$, and consists of 769 (3030) galaxies with magnitude $m_z \leq 14.5$ (15.5) and redshift $cz \leq 17000$ (27000) km s^{-1} . For comparison, the previously analyzed subsamples of CfA1 N+S, SSRS1, and CfA2 Slices, are characterized respectively by: $\omega = 1.83 + 0.83, 1.75, 0.42 \text{ sr}$, $m_Z \leq 14.5, \approx 14.5$ (apparent-diameter-limited), 15.5 , $N_g = 1534, 1845 + 556, 1766$.

The characteristics of all group catalogs are listed in Table 1. The two significative cases TB96₁ and TB96₂ (in PPS1 and PPS2, respectively) are also shown in Fig. 1 (bottom panels). Groups are identified with the friends-of-friends algorithms described in TB96, both HG-like (HG82) and NW-like (NW87). Briefly, two galaxies closer then some specified

transverse separation D_L and radial separation V_L in redshift space are friends of each other. Friendship is transitive, and a galaxy group is an isolated set of friends. The two links are normalized by D_0 and V_0 at a given fiducial redshift (here $cz_0 = 1000 \text{ km s}^{-1}$), and are then scaled-up with cz , using the selection function

$$\psi(cz; m_{lim}) = \frac{\int_{-\infty}^{M_{lim}} dM \phi(M)}{\int_{-\infty}^{M_{fai}} dM \phi(M)}. \quad (2)$$

Here m_{lim} is the apparent-magnitude limit of the sample, $\phi(M)$ is the galaxy luminosity function, M_{fai} is the faintest absolute magnitude in the sample, while the dependence on m_{lim} and cz arises through

$$M_{lim} = m_{lim} - 25 - 5 \log_{10}(cz/H_0). \quad (3)$$

To scale up the links, the original HG prescription (based on simple arguments, Monte-Carlo tested) gives $D_L \propto V_L \propto \psi(cz)^{-1/3}$, while the NW recipes (based and tested on N-body simulations) takes $D_L(cz) \propto (cz)^{-1/3} \psi(cz)^{-1/2}$, and $V_L = V_0 + b \cdot (cz - cz_0)$, where cz is the mean redshift of the pair of galaxies considered, and $b = 0.030$ is a suitable constant (for a detailed discussion of the reasons behind such different choices, see TB96 and the references therein). The value of D_0 corresponds to an effective density threshold (in redshift space), given by

$$1 + \frac{\delta n}{n} = \left[\frac{4\pi}{3} D_0^3 \int_{-\infty}^{M_{lim}} dM \phi(M) \right]^{-1} \quad (4)$$

We adopt the galaxy luminosity function in the Schechter (1976) form determined from PPS2 by TB96 ($\alpha = -1.15$, $M_* = -19.30$; here we take $\phi_* = 0.020 h^3 \text{Mpc}^{-3}$). The number of groups in all catalogs is approximately $N_G = 0.06 \cdot N_g \propto \omega 10^{m_{lim}}$, i.e. $N_G \sim 200$ in PPS2 and $N_G \sim 50$ in PPS1. For sake of comparison, $N_G = 88 + 47,87$, and 128 in JZ88, MdC90, and RGH90 respectively. It is clear that the characteristics of each groups catalogue are fixed, to some extent, by the choice of parameters in the identification

algorithm. Smaller values of the links D_0 and V_0 yield groups with higher density contrast and, within biased theories of galaxy formation, this is expected to cause a stronger spatial correlation. As outlined in TB96, a similar effect arises from the sample depth. This subtler point requires some explanation. It is clear that the increase of the mean galaxy density, which occurs when the magnitude limit passes from m_{lim}' to $m_{lim}'' > m_{lim}'$, is accounted for by a slower decrease of the selection function with cz . In fact, eq. 3 shows that $\psi(m_{lim}''; cz'') = \psi(m_{lim}'; cz')$, provided that $cz'' = cz' 10^{m_{lim}'' - m_{lim}'}$; accordingly, everything which happened at cz' is now moved to cz'' , in the deeper sample. Everything is therefore scaled, apart of cz_0 , the redshift value where the sky-link D_L is normalized.

Normalizing at the *same* location $cz_0 = 1000 \text{ km s}^{-1}$ for *different* m_{lim} 's yields different density contrasts $\delta n/n$ for the same value D_0 . Groups identified with the same values of D_0 and V_0 are then expected to be more correlated in PPS1 than in PPS2.

An analogous effect is expected for the redshift-link V_L , though different for the HG and NW algorithms. In fact, RGH90 suggested that the different values JZ88 and Mdc90 adopted for V_0 could account for the discrepancies from their results, but they did not take into account the stronger effect presumably arising from the different m_{lim} . (The effects of changing m_{lim} , D_0 , and V_0 , are shown in Fig. 5; a much more detailed discussion will be provided in Sect. 4.)

It is also important to outline that giving the D_0 link is not immediately equivalent to providing a threshold density contrast. According to eq. (4), $\delta n/n \propto \phi_* D_0^3$, but ϕ_* variations by a factor of 2 can arise both from observational techniques and/or local physical conditions. The other parameters determining the Schechter function, adopted by RGH89 and F95, and worked out by dLGH88 ($\alpha = -1.2$, $M_* = -19.15$) are almost consistent with those worked out from our sample. TB96 showed that, for similar changes ($\Delta\alpha = \pm 0.1$ and $\Delta M_* = 0.1$), the net effect on the internal properties of output groups is

small. Furthermore, the spatial distribution of groups is almost insensitive even to greater differences in the identification algorithm.

As shown by dLGH88 and Martinez et al. (1993), estimates of $\xi(r)$ are sensitive to the presence of large scale features in the samples. In the present analysis, we cut *all* samples within $cz \leq 11000 \text{ km s}^{-1}$. The number of groups does not change in PPS1 (767 galaxies), while it is reduced by $\sim 5\text{--}10\%$ in PPS2 (2693 galaxies). This cut-off ensures that we are always dealing with the same physical structures, though differently sampled by different m_{lim} 's. The same main LSS features are present in both galaxy samples, and they are reflected on the spatial distribution of groups (Fig. 1).

3. Two-point functions for galaxies and groups: estimate and errors

Let us now describe the procedure leading to the 2-point function estimate. As usual, we center spherical shells of radius r and width δr on each observed object in the data (D : galaxy/group) sample. We then count neighbours in the data sample and in a random control sample, spatially uniform but with the same shape and radial selection function as the data. To do so, \tilde{N}_R random points are taken from a spatially uniform distribution with the same shape of the data sample, but they are weighted down by the selection function $\psi(cz; m_{lim})$. In particular, the total number of random points \tilde{N}_R is replaced by the total weight $N_R = \sum_{k=1}^{\tilde{N}_R} w_k$, where $w_k = \psi(cz_k; m_{lim})$ is the weight of the k -th random point. We then divide the number $DD(r; j)$ of (observed) neighbour objects within $r \pm \delta r/2$ by the (weighted down) number $DR(r; j)$ of neighbour random points, and then average over all N_D centers. Our weighting scheme is analogous to that of the ξ_{11} estimator discussed in dLGH88 (see also Martinez et al. 1993). Altogether, this amounts to estimating $\xi(r)$

through the following formula, that we use both for groups and galaxies:

$$1 + \xi(r) = \langle 1 + \xi(r; j) \rangle_{j=1, \dots, N_D} = \frac{1}{N_D} \sum_{j=1}^{N_D} \frac{DD(r; j)}{DR(r; j)} \frac{N_R}{N_D} \quad (5)$$

We adopt the same selection functions for galaxies and groups, by using both in PPS1 and PPS2 the luminosity function $\phi_{STY}(M)$ evaluated in TB96 from PPS2 (in some cases, we use also $\phi(M)$ from dLGH88). In fact, the radial distribution of galaxies and groups substantially agree over the relevant redshift range (see Fig. 2).

Errorbars are computed with 10 bootstrap resampling of the data (Barrow, Bhavsar, & Sonoda 1984). Bootstrap errors are expected to overestimate the true ensemble errors, in turn larger than formal Poisson errors. The ratio between bootstrap and Poisson errors is expected to be ~ 1.6 – 2.6 (Martinez et al. 1993), with a slight dependence on r and data depth. On the other hand, weighting data by $(1/\text{bootstrap errorbar})^2$ in the least-squares fit of $\xi(r)$ to $Ar^{-\gamma}$, and simultaneously treating r -bins as independent, tends to compensate the bootstrap overestimate, yielding fair values for $A \pm \Delta A$ and $\gamma \pm \Delta\gamma$ (e.g., Ling, Frenk, & Barrow 1986).

4. Results and Discuss

Plots of 2-point correlation functions for groups are given in Figs. 3a and b. For the sake of comparison, in each Figure, the galaxy 2-point functions are from the same sample also plotted. Here, groups are identified with $D_0 = 0.27 h^{-1}\text{Mpc}$ and $V_0 = 350 \text{ km s}^{-1}$, as in RGH89. Bootstrap error bars are given for all points. A least-square bootstrap-weighted fit to $\xi(r) = Ar^{-\gamma}$ is then performed. The best fit A and γ and their errors are listed in Tables 2 and 3 for PPS1 and PPS2, respectively. For galaxies the fits can be extended from 1 to $31.7 h^{-1}\text{Mpc}$. For groups, instead, the most reasonable distance interval is from 1.5 to $10 h^{-1}\text{Mpc}$. For $r/h^{-1}\text{Mpc} < 1.5$ anti-correlation due to the intrinsical size of groups is

expected to (and does) take over. The plots also show that, for $r/h^{-1}\text{Mpc} > 10$ the signal is too noisy to be of any use. This distance interval is similar to those used in previous group correlation analyses. We however performed fits both for galaxies and groups in both kinds of distance intervals.

From Fig. 3 we see that, although (1) within $2\text{-}\sigma$ bootstrap errorbars, $\xi_{GG} \approx \xi_{gg}$, (2) ξ_{GG} is mostly *higher* than ξ_{gg} by a factor $\gtrsim 2$. Accordingly, from Tables 2 and 3, we see that A_G systematically exceeds A_g . For the narrower and most reliable distance range, $A_G/A_g \sim 3$ for PPS1, and $A_G/A_g \sim 2$ for PPS2. In this two-parameter fit, the amplitudes are different at the $\sim 2.5\text{-}\sigma$ level, but their difference has the same sign anywhere, and can be suspected to be real. Also the slope γ of groups is however greater than the corresponding slope of galaxies. Let us just remind that the range of γ 's found here is not unusual in the redshift space and, for galaxies, corresponds to steeper $\tilde{\gamma}$'s in the range 1.6–1.9 in the real space (e.g., Gramann, Cen, & Bahcall 1993). The shift from redshift to real space is clearly expected to be weaker for groups. It is not clear to which extent this can justify the steeper γ found for groups; this effect exceeds $2\text{-}\sigma$'s for PPS1 only, but is present anywhere. With a comparable level of confidence we also see that: (3) A_G for PPS1 exceeds A_G for PPS2 by more than 50%, while, in the same (narrower) distance range A_g for PPS1 and PPS2 are almost consistent within $1\text{-}\sigma$. However, for galaxies, we can exploit the wider distance range, and there we find a probable signal of luminosity segregation at the $3\text{-}\sigma$ level.

The point (1) was also outlined by RGH90 in CfA2 Slices, while the point (2) is in contrast with RGH90, MdC89, and JZ88. Let us however remark that JZ88 and MdC89 used much larger D_0 's than us and RGH90. Adopting the same links and $\phi(L)$ parameters as for JZ88's groups (GH83), we obtain much lower and noisier ξ_{GG} 's, both for PPS1 and PPS2. This is shown in Fig. 4a, where, at variance with JZ88, error bars are also provided. The discrepancy with RGH90, instead, is less pronounced. Besides of using a different data

set, RGH90 make also use of different $\phi(L)$ parameters. If we make use of such parameters to detect groups in PPS2 we obtain a lower ξ_{GG} , nearly overlapping ξ_{gg} (compare Fig. 3b and Fig. 4b).

An attractive interpretation of point (2) is a *relative* segregation of groups with respect to galaxies. A similar effect between halos and halo groups in N-body simulations of flat unbiased CDM (Gelb 1992) was found by F95, who however showed that this result can depend on the identification scheme. Although bearing in mind such reserves, we agree with F95 that RGH90’s outputs conflict with flat unbiased CDM models. However, this conflict is not evident in our outputs.

As already outlined, the obvious interpretation of the point (3) for galaxies is luminosity segregation: as first shown by Davis et al. (1988) and convincingly demonstrated by Park et al. (1994) using complete *volume-limited* samples, brighter galaxies are more clustered than fainter one. This can be related to their greater luminosity either directly (e.g., Hamilton 1988; Hollosi & Efstathiou 1988; Davis et al. 1988; Gramann & Einasto 1992) or through the luminosity–morphology connection (e.g., Iovino et al. 1993; Hasegawa & Umemura 1993). Such effect is also predicted by theoretical scenarios (e.g., White et al. 1987; Bonometto & Scaramella 1988; Valls-Gabaud, Alimi, & Blanchard 1989) and a similar effect of *mass* segregation has been found in large N-body simulations (e.g., Campos et al. 1995).

Independently of the interpretation, it is clear that cutting both PPS1 and PPS2 within the *same* limit $cz_{cut} = 11000 \text{ km s}^{-1}$, PPS1 contains all the brighter galaxies of PPS2 because of the brighter m_{lim} . For these *incomplete* samples, limited both in cz and in m , we expect ξ_{gg} to be greater for brighter m_{lim} . On the contrary, for *complete* apparent–magnitude limited samples (cz_{cut} increasing with m_{lim}), we expect ξ_{gg} to be greater for fainter m_{lim} (e.g., Hamilton 1988), as the total number of intrinsically bright

galaxies in such samples increases with fainter m_{lim} and dominates the sample.

A possible interpretation of the point (3) for groups is that, in PPS1, we selected higher density contrast groups than in PPS2. In fact, using the same D_0 for both PPS1 and PPS2, while the mean inter galaxy separation is smaller for fainter m_{lim} , can enhance the correlation in PPS1. But this effect might not be enough. In fact we checked that the change of D_0 in either PPS1 or PPS2 has smaller effects than passing from PPS1 to PPS2. This is shown in Fig. 5a and b, where we give ξ_{GG} for groups selected in 2 different ways both in PPS1 and PPS2. Using $D_0 = 0.24h^{-1}\text{Mpc}$ ($D_0 = 0.30h^{-1}\text{Mpc}$) in PPS2 (PPS1) we have the same $\delta n/n$ that $D_0 = 0.27h^{-1}\text{Mpc}$ gives in PPS1 (PPS2). The changes of ξ_{GG} are however slight within either PPS1 or PPS2, in spite of the change of D_0 .

We explore further the dependence of ξ_{GG} on D_0 in Fig. 5c. As expected, ξ_{GG} increases with $\delta n/n$ within a given sample (the Figure refers to PPS2). In Fig. 5d, instead, we test the dependence on V_0 and discover that, at variance with what could be expected, ξ_{GG} does not depend on V_0 , in spite of varying the redshift link over a greater range than D_0 . As a further check, we also used the NW scaling recipe, whose V_L has a quite different shape from the HG scaling (D_L 's are very similar). No effect on ξ_{GG} is however present. (This agrees with F95, and is consistent with TB96 who showed how for given self-consistent normalizations and different scaling recipes the spatial distribution of HG-like and NW-like groups is very similar.) It is difficult to comment on this point, which however seems to indicate that varying V_0 is not so effective to change the density contrast and that the redshift link is therefore less *physical* than the sky link. In fact, TB96 showed how a restrictive V_L affect groups more as a cut-off (discarding high-velocity-dispersion systems) than as a systematic variation of the properties of each single group. On the other hand, changing D_L directly affects $\delta n/n$ of the output groups. From a physical point of view, this might suggest that clustering of galaxy systems is more directly related to their density

contrast than to their velocity dispersion (mass?).

Note that groups are on average brighter in PPS1 than in PPS2 (TB96). A natural interpretation of point (3) could be luminosity (mass?) segregation among *groups* themselves. But this could be a premature conclusion. In fact, in order to compare group luminosity the *observed* group luminosity L_{obs} should be implemented by L_{fai} for group members below m_{lim} . But this correction depends on several assumptions (Mezzetti et al. 1985; Gourgoulhon, Chamaraux, & Fouqu e 1992; Moore et al. 1993). The enhancement of ξ_{GG} in PPS1 could be just an effect of a higher correlation of group members. In fact, groups are brighter in PPS1 than in PPS2 because their *members* are. Henceforth, luminosity segregation of *galaxies*, not of groups themselves.

However, Fig. 1 shows that the relatively nearby main ridge in PPS at $cz \approx 5000 \text{ km s}^{-1}$ is equally well sampled in both PPS1 and PPS2, while the more sparsely populated region between 6000 and 11000 km s^{-1} in PPS2 is completely devoid of groups in PPS1. From this point of view, groups *are* indeed more clustered in PPS1 than in PPS2, but simply because of “cosmographical” reasons, not because of their higher luminosity. Therefore, an explanation of effect (3) could be an intrinsic difference in the data sets PPS1 and PPS2.

Previous analyses of group clustering (JZ88, MdC90, RGH90) led to apparently contradictory results. The main source of discrepancy lies in the different search parameters of the adaptive Friends–Of-Friends algorithms adopted by various authors. The greater difference is due to the transverse normalization D_0 . Stricter D_L ’s yield stronger correlations, thus explaining the discrepancy among JZ88 on one side ($\xi_{gg} \approx 2.5\xi_{GG}$) and RGH90 on the other ($\xi_{gg} \approx \xi_{GG}$). Instead, contrary to simple expectation, no dependence on the radial link V_L (as suggested by RGH90) is detected. A further reason of difference is the impact on group properties of the different depth of the adopted samples. This effect (partially considered by RGH89 and MdCL89, but not by RGH90 and MdC90)

requires a suitable handling of the “parameter” m_{lim} in the identification algorithm, and a self-consistent normalization of D_L . Simply adopting the same value of D_0 leads to lower density contrasts in shallower samples, also contributing to the shallower ξ_{GG} of JZ88 and MdC90. The residual difference among samples of different depth is nevertheless more important. This is the case for the samples PPS1 and PPS2, and an analogous effect was pointed out by RGH89 for CfA1 Survey and CfA2 Slices. A further reason of discrepancy between RGH90 and MdC90 could be the different physical nature of the CfA and SSRS samples. As shown by MdCL89, groups in CfA1 and SSRS1 have similar physical properties when *different* values of the links are used. In fact, the former survey contains a higher percentage of early-type galaxies, in general more clustered than the late-type galaxies in the latter.

5. Conclusions

The attention devoted by a number of authors to the clustering of loose groups is widely justified. Galaxies and clusters are both clustered, but their clustering parameters are different. The discovery of such difference was the original motivation to introduce the biased theory of galaxy formation. An independent test of such theory as a whole and a further constraint on its parameters arise from a sufficiently precise determination of clustering parameters of groups.

To pursue this program we need an unambiguous definition of loose groups and a sample wide enough to test their properties. In the literature there has been a complex debate on group individuation, which is technically provided by suitable sky link (D_L) and redshift link (V_L), in transverse and radial direction, respectively. This is due to the need of exploiting the whole information contained in apparent magnitude limited samples, and overcoming the critical problem of distortions due to the passage from the redshift to the

real space.

This work shows that results on clustering parameters, obtained with different group individuation recipes, are essentially consistent. This does not mean that the values of the links do not matter. On the contrary, the clustering strength is critically dependent on how restrictive the selection is. The point is that D_L has a stronger impact on clustering properties than V_L . Different criteria (e.g., NW vs. HG) are essentially different as far as the radial link V_L is concerned, but the effect on $\xi(r)$ of fairly wide variations of V_L is negligible, while smaller variations of D_L are reflected on the clustering of groups.

To some extent, this is a natural outcome of working in *redshift space*. The transverse link D_L is directly related to the spatial separation among group members. In the radial direction, instead, peculiar velocities inside groups yield ambiguous apparent separations. Relating V_L to a value of $\delta n/n$ is then not trivial and depends on the cosmological model (e.g., NW87).

This problem would be present even if we could select a complete volume-limited galaxy sample, and then identify groups therein as suggested by Ramella et al. (1995a,b). (Selecting volume-limited subsamples of the group catalogs *after* group identification with the adaptive HG and NW algorithms (Zabludoff et al. 1993a,b), is not the ideally correct solution, as groups could be already biased by the magnitude-limited nature of the galaxy data source.) Unfortunately, to be really efficient, this procedure requires a high number of measured redshifts. *E.g.*, even adopting the *generous* constant links $D_0 = 0.5 h^{-1}\text{Mpc}$, $V_0 = 350 \text{ km s}^{-1}$, volume limiting PPS2 to $cz \leq 7900 \text{ km s}^{-1}$ ($M \leq -19.5$) as in Guzzo et al. (1991) and Bonometto et al. (1993) yields only $N_G \approx 50$ groups, and it is not sure that this is enough.

Resorting then to *apparent-magnitude-limited* samples, two further but connected source of complication arise. First, the physical mixture of what we consider *bright* and

faint galaxies varies with redshift. Second, the mean separation among observed galaxies grows with cz , and group identification is harder at higher redshifts. To some extent, the traditional strategy of compensating the decrease of galaxy density by scaling up D_L and V_L , gives group properties doomed to be systematically dependent on cz (and, to a lesser extent, to the scaling recipe and galaxy luminosity function).

Previous analyses of group clustering (JZ88, MdC90, RGH90) in CfA and SSRS surveys led to apparently contradictory results. In this paper, we have investigated the source of such discrepancies, finding satisfactory explanations for them. Together with that, we have found a signal of group clustering, whose amplitude exceeds the amplitude of galaxy clustering. Such excess is perhaps to be trusted more than what its formal probability ($\sim 2.5\sigma$'s) prescribes, as it persists through various density contrasts and link recipes; it could be found mostly thanks to the wider extension of PPS in respect to the sample used for previous analyses.

We are grateful to R. Giovanelli and M. P. Haynes for discussions, and for kindly providing us with the PPS data.

Table 1. FOF algorithms and group catalogs.

Group Catalog	D_0	V_0	$\delta n/n$	Number of groups
TB96 _{1,2}	0.27	350	160,110	48, 192
wide ₁	0.30	350	110, ...	48, ...
strict ₂	0.24	350	..., 160	..., 179
high _{1,2}	0.21	350	330, 240	40, 168
low _{1,2}	0.42	350	40, 30	59, 205
cold _{1,2}	0.27	150	160, 110	43, 186
hot _{1,2}	0.27	600	160, 110	50, 201
TB96NW _{1,2}	0.27	350	160, 110	48, 162
RGH89 _{1,2}	0.27	350	120, 80	49, 192
RGH83 _{1,2}	0.27	600	120, 80	52, 205
DGH83 _{1,2}	0.52	600	16, 10	60, 185

Note. — Indexes 1, 2 stand for the galaxy samples PPS1, PPS2 where groups are drawn from. Scaling recipes are everywhere as in HG82, except for TB96NW as in NW87. The reference algorithm TB96 is detailed as follows: wide₁/strict₂ means wide/strict D_0 (in h^{-1} Mpc), so to match $\delta n/n$ of the samples TB96₂, TB96₁ respectively (see text); high/low means high/low density contrast $\delta n/n$, i.e. small/large D_0 ; cold/hot means low/high velocity dispersion σ_v , i.e. small/large V_0 (in km s^{-1}). The galaxy luminosity function is everywhere as in TB96, except for RGH89, RGH83, and DGH83

Table 2. A and γ for groups and galaxies in PPS1.

Sample	$\gamma \pm \Delta\gamma$	$A \pm \Delta A$	$r_0 \pm \Delta r_0$
PPS1	$1.21 \pm .04$	$10.54 + .75 - .70$	$7.03 + 0.62 - 0.60$
TB96 ₁	$1.32 \pm .16$	$24.2 + 6.4 - 5.0$	$11.2 + 4.0 - 3.8$
PPS1	$1.08 \pm .06$	$9.5 + 0.9 - 0.8$	$8.0 + 1.2 - 1.1$
TB96 ₁	$1.39 \pm .26$	$30.2 + 15 - 9.8$	$11.6 + 6.6 - 5.9$
wide ₁	$1.50 \pm .29$	$42 + 23 - 15$	$12.0 + 7.2 - 6.4$
high ₁	$1.32 \pm .32$	$41 + 25 - 16$	$17 + 14 - 13$
low ₁	$1.20 \pm .28$	$11.3 + 5.4 - 3.6$	$7.5 + 4.6 - 4.0$
NW ₁	0.70 ± 1.25	$10.0 + 5.3 - 3.5$	$27 + 37 - 34$
cold ₁	1.26 ± 0.28	$26.4 + 13 - 8.5$	$13.4 + 9.3 - 8.5$
hot ₁	1.51 ± 0.33	$44 + 30 - 18$	$12.5 + 8.8 - 7.6$
RGH89 ₁	$1.59 \pm .28$	$50 + 27 - 18$	$11.7 + 6.5 - 5.7$
RGH83 ₁	$1.36 \pm .25$	$43 + 20 - 14$	$16.0 + 10 - 9.1$
DGH83 ₁	$0.67 \pm .74$	$2.0 + 5.3 - 1.5$	$3.9 + 12 - 5.0$

Note. — Two-parameters least-square fit of $\xi(r) = Ar^{-\gamma}$ to galaxy and group data (within the same sample); 1- σ bootstrap errors are provided. In the first two lines the distance range $1.0 \leq hr/\text{Mpc} \leq 31.7$ is considered. In the other lines $1.5 \leq hr/\text{Mpc} \leq 10.0$. The wider interval is actually suitable to fit the 2-point function for galaxies only (see text). Different group catalogs are obtained from different grouping criteria (see text and Table 1), but the most significant outputs are the 1st and 4th lines (marked in bold characters).

Table 3. A and γ for groups and galaxies in PPS2.

Sample	$\gamma \pm \Delta\gamma$	$A \pm \Delta A$	$r_0 \pm \Delta r_0$
PPS2	$1.26 \pm .02$	$7.42 + .20 - .19$	$4.92 + .18 - .17$
TB96 ₂	$1.31 \pm .14$	$12.5 + 2.9 - 2.3$	$6.9 + 1.8 - 1.7$
PPS2	$1.21 \pm .04$	$7.65 + .36 - .34$	$5.36 + .35 - .34$
TB96₂	$1.36 \pm .19$	$14.5 + 3.8 - 3.0$	$7.2 + 2.5 - 2.2$
strict ₂	$1.37 \pm .18$	$15.4 + 4.4 - 3.4$	$7.3 + 2.4 - 2.2$
high ₂	$1.04 \pm .19$	$9.2 + 3.1 - 2.3$	$8.6 + 4.4 - 4.0$
low ₂	$1.58 \pm .23$	$9.5 + 3.2 - 2.4$	$4.1 + 1.2 - 1.1$
NW ₂	$1.08 \pm .19$	$9.4 + 3.4 - 2.5$	$7.9 + 3.9 - 3.5$
cold ₂	$1.28 \pm .13$	$14.0 + 2.5 - 2.1$	$7.9 + 2.0 - 1.9$
hot ₂	$1.29 \pm .22$	$13.5 + 5.6 - 4.0$	$7.5 + 3.5 - 3.1$
RGH89 ₂	$1.63 \pm .23$	$16.0 + 5.5 - 4.1$	$5.5 + 1.7 - 1.6$
RGH83 ₂	$1.45 \pm .24$	$12.7 + 5.0 - 3.6$	$5.8 + 2.3 - 2.0$
DGH83 ₂	$0.83 \pm .38$	$1.9 + 1.6 - 0.9$	$2.2 + 2.3 - 1.4$

Note. — Same as for Table 2, but for galaxies and groups in PPS2. The comparison of the two bold face lines (1st and 4th) yields one of the main results of this paper.

REFERENCES

- Abell G.O., 1958, ApJS 3, 211
- Abell G.O., Corwin H.C., & Olowin R.P., 1989, ApJS 70, 1
- Bahcall, N. A., & Soneira, R. M., 1983, ApJ 270, 20
- Barrow, J. D., Bhavsar, S. P., & Sonoda, D.H. 1984, MNRAS 210, 19p
- Bonometto, S. A., & Scaramella, R. 1988, preprint, submitted to A&A
- Bonometto, S. A., Iovino, A., Guzzo, L., Giovanelli, R., & Haynes, M. P., 1993, ApJ 419, 451
- Borgani S., 1995, Phys.Rep. 251, 1
- Borgani S., et al. 1995, MNRAS 277, 1191
- Burstein, D., & Heiles, C., 1978, ApJ 225, 40
- Campos, A., Yepes, G., Klypin, A., Murante, G., Provenzale, A., & Borgani, S., 1995, ApJ 446, 54
- da Costa, L. N., Pellegrini, P. S., Sargent, W. L. W., et al. 1988, ApJ 327, 544
- Dalton, G. B., Efstathiou, G., Maddox, S. J., & Sutherland, W. J., 1992, ApJ 390, L1
- Davis, M., & Huchra, J. P., 1982, ApJ 254, 437
- Davis, M., & Huchra, J. P., Latham, D. W., & Tonry, J., 1982, ApJ 253, 423
- Davis, M., Meiksin, A., Strauss, M. A., daCosta, L. N. & Yahil, A., 1988, ApJ 333, L9
- de Lapparent, V., Geller, M. J., & Huchra, J. P., 1988, ApJ 302, L1 (dLGH86)

- de Lapparent, V., Geller, M. J., & Huchra, J. P., 1988, ApJ 332, 88 (dLGH88)
- de Lapparent, V., Geller, M. J., & Huchra, J. P., 1989, ApJ 343, 117 (dLGH89)
- Frederic, J. J., 1995, ApJS 97, 259 (F95a)
- Frederic, J. J., 1995, ApJS 97, 275 (F95b)
- Gelb, J. M., 1992, M.I.T. Ph.D. Dissertation
- Geller, M. J., & Huchra, J. P., 1983, ApJS 52, 61 (GH83)
- Geller, M. J., & Huchra, J. P., 1989, Sci 246, 897
- Ghigna, S., Borgani, S., Bonometto, S. A., et al., 1994, ApJ 437, L71
- Giovanelli, R., Haynes, M. P., & Chincarini, G., 1986, ApJ 300, 77
- Giovanelli, R., & Haynes, M. P., 1989, AJ 97, 633
- Giovanelli, R., & Haynes, M. P., 1991, ARA&A 29, 499
- Giovanelli, R., & Haynes, M. P., 1993, AJ 105, 1271
- Gourgoulhon, E., Chamaraux, P., & Fouquè, P., 1992, A&AS 255, 69
- Gramann, M., & Einasto, J., 1992, MNRAS 254, 453
- Gramann, M., Cen, R., & Bahcall N.A. 1993, ApJ 419, 440
- Guzzo, L., Iovino, A., Chincarini, G., Giovanelli, R., & Haynes, M. P., 1991, ApJ 382, L5
- Hamilton, A. J. S., 1988, ApJ 331, L59
- Haynes, M. P., Giovanelli, R., Starosta, B., & Magri C.A., 1988, AJ 95, 607
- Hasegawa, T., & Umemura, M., 1993, MNRAS 263, 191

- Hollosi, J., Efstathiou, G., 1988, “Large Scale Structure in the Universe”, Springer–Verlag
- Huchra, J. P., & Geller, M. J., 1982, ApJ 257, 423 (HG82)
- Huchra, J. P., Davis, M., Latham, D., & Tonry, J., 1983, ApJS 52, 89
- Huchra, J. P., Geller, M. J., de Lapparent, V., & Corwin, H. G. Jr., 1990, ApJS 72, 433
- Huchra, J. P., Geller, M. J., & Corwin, H. G. Jr., 1995, ApJS 99, 391
- Iovino, A., Giovanelli, R., Haynes, M., Chincarini, G., & Guzzo, L., 1993, MNRAS 265, 21
- Jing, Y., & Zhang, J., 1988, A&A 190, L21 (JZ88)
- Kaiser, N., 1984, ApJ 284, L9
- Kashlinsky, A., 1987, ApJ 317, 19
- Klypin, A. A., Holtzmann, J., Primack, J. R., & Regös E., 1993, ApJ 416, 1
- Klypin, A. A., & Kopylov, A. I. 1983, Sov.Astron.Lett. 9, 41
- Klypin, A. A., Nolthenius, R., & Primack, J. R., 1995, ApJ submitted, astro-ph 9502062
- Ling, E.N., Frenk, C.S., & Barrow, J. D., 1986, MNRAS 223, 21p
- Maia, M. A. G., da Costa, L. N., & Latham, D. W., 1989, ApJS 69, 809 (MdCL89)
- Maia, M. A. G., & da Costa, L. N., 1990, ApJ 349, 477 (MdC90)
- Martinez, V. J., Portilla, M., Jones, B. J. T., & Paredes, S. 1993, A&A 280, 5
- Mezzetti, M., Pisani, A., Giuricin, G., & Mardirossian, F. 1985, A&A 143, 188
- Moore, B., Frenk, C. S., & White, S. D. M., 1993, MNRAS 261, 827
- Nichol, R. C., Collins, C. A., Guzzo, L., & Lumsden, S. L.’ 1992, MNRAS 255, 21

- Nichol, R. C., Briel, U. G., Henry, J. P., 1994, MNRAS 265, 867
- Nolthenius, R., Klypin, A. A., & Primack, J. R., 1994, ApJ 422, L25 (NKP94)
- Nolthenius, R., Klypin, A. A., & Primack, J. R., 1995, ApJ submitted, astro-ph 9410095 (NKP95)
- Nolthenius, R., & White, S., 1987, MNRAS 225, 505 (NW87)
- Park, C., Vogele, M. S., Geller, M. J., & Huchra, J. P., 1994, ApJ 431, 569
- Peebles, P. J. E., 1980, “The Large Scale Structure of the Universe”, Princeton University Press
- Politzer, H. D., Wise, M. D. 1984, ApJ 285, L1
- Prandoni, I., Iovino, A., & MacGillivray, H. T., 1994, AJ 107, 1235
- Ramella, M., Geller, M. J., & Huchra, J. P., 1989, ApJ 344, 57 (RGH89)
- Ramella, M., Geller, M. J., & Huchra, J. P., 1990, ApJ 353, 51 (RGH90)
- Ramella, M., Geller, M. J., Huchra, J. P., & Thorstensen, J. R. 1995a, AJ 109, 1458
- Ramella, M., Geller, M. J., Huchra, J. P., & Thorstensen J.R. 1995b, AJ 109, 1469
- Sahni P., & Coles P., 1995, Phys Rep. D 262, 1
- Schechter, P., 1976, ApJ 203, 297
- Sutherland, W. J., 1988, MNRAS 234, 159
- Trasarti Battistoni, R., 1995, Ph.D. Dissertation, Università degli Studi di Milano, Italia
- Trasarti Battistoni, R., 1996, A&A submitted

Valls–Gabaud, D., Alimi, J. M., & Blanchard, A. 1989, *Nature* 341, 215

Wegner, G., Haynes, M.P., & Giovanelli, R., 1993, *AJ* 105, 1251

White, S. D. M., Frenk, C. S., Davis, M., & Efstathiou, G., 1987, *ApJ* 313, 505

Yahil, A., Tamman, G. A., & Sandage, A., 1977, *ApJ* 217, 903

Zabludoff A., Geller M.J., Huchra J.P., & Vogeley M.S. 1993a, *AJ* 106, 1273

Zabludoff, A. I., Geller, M. J., Huchra, J. P., & Ramella, M., 1993b, *AJ* 106, 1301

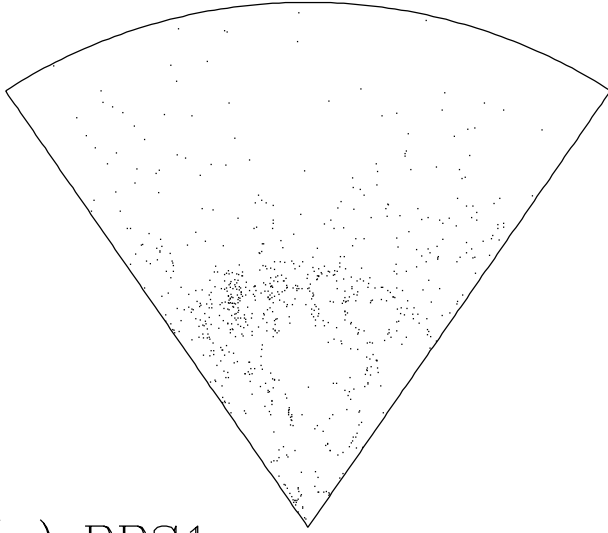
Fig. 1.— Wedge diagrams (α - cz) of galaxies and loose groups in the Perseus–Pisces redshift Survey (only the region with low galactic extinction $-1.5^h \leq \alpha \leq +3.0^h$, $0^\circ \leq \delta \leq +40^\circ$; all samples are cut within $cz_{cut} = 11000 \text{ km s}^{-1}$). Groups are identified with the adaptive Friends–Of–Friends algorithm of Huchra & Geller (1982) (for definitions, see text). (a) Galaxy sample PPS1. (b) Galaxy sample PPS2. (c) Group sample TB96₁. (d) Group sample TB96₂.

Fig. 2.— Ratio dN_G/dN_g between the number dN_G of (identified) groups and the number dN_g of (observed) galaxies in the galaxy sample PPS2. Three typical cases (with different search parameters D_0 , V_0 , and $\phi(L)$ – see Table 1) are shown. Within the relevant distance range $2000 \lesssim cz/\text{km s}^{-1} \lesssim 10000$, the radial distribution of groups and galaxies are in good agreement – i.e., groups and galaxies share the same radial selection function ($dN_G/dN_g \sim 1/15$ independently of cz).

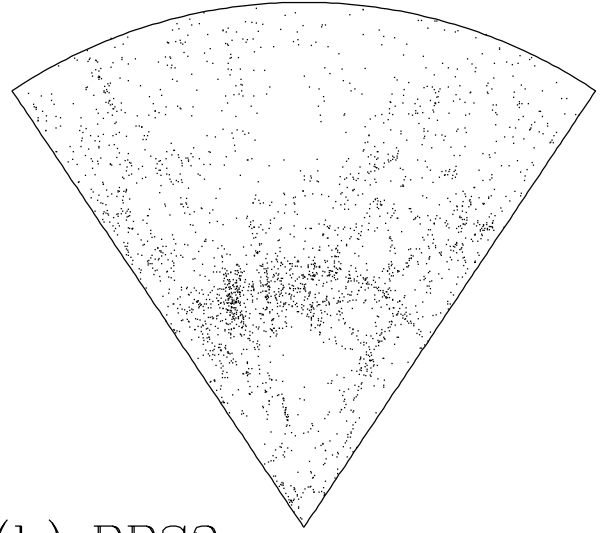
Fig. 3.— Two–point correlation functions $\xi_{GG}(r)$ for loose groups (thick lines) and $\xi_{gg}(r)$ for galaxies (thin lines), within the *same* galaxy sample(s): (a) PPS1; (b) PPS2. Errorbars are $\pm 1\text{-}\sigma$ bootstrap. In both samples, $\xi_{GG} \gtrsim 2\xi_{gg}$ systematically, though $\xi_{GG} \approx \xi_{gg}$ within $2\text{-}\sigma$ errorbars. Also, both $\xi_{gg}(r)$ and $\xi_{GG}(r)$ in PPS1 are slightly *higher* than in PPS2.

Fig. 4.— Comparison of $\xi_{GG}(r)$ in PPS2 for the loose group sample TB96₂ and other samples identified as in previous analyses: (a) As in JZ88 ($D_0 = 0.52$, $V_0 = 600$ as in GH83; $\phi(L)$ as in RGH89), for both PPS1 and PPS2; (b) As in RGH89/90 ($D_0 = 0.27$, $V_0 = 350$; $\phi(L)$ as in RGH89), for PPS2. (The parameters of TB96₂ are: $D_0 = 0.27$, $V_0 = 350$, and $\phi(L)$ as in TB96.) The high noise in DGH83₁ is partially due to the low number of groups ($N_G = 60$), but the same degree of noise is also present in DGH83₂ ($N_G = 185$). The errorbars of RGH89₂ are similar to (but sometimes larger than) those of TB96₂, though $N_G = 192$ in both cases. Compare the small effect of $\phi(L)$ with those due to D_0 and m_{lim} (see Fig. 5).

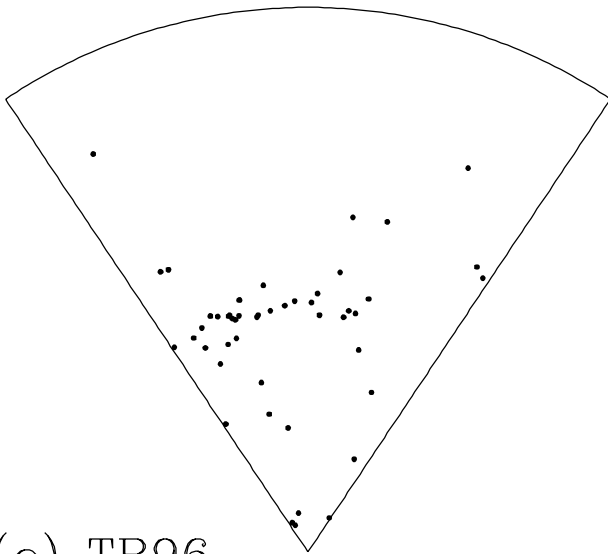
Fig. 5.— Dependence of $\xi_{GG}(r)$ in PPS1/PPS2 on m_{lim} , $\delta n/n$, D_0 , and V_0 (scaling recipe as in HG82, $\phi(L)$ from TB96 – see text): (a) TB96₁ with the “standard” $D_0 = 0.27$, and the “renormalized” $D_0 = 0.30$ (wide₁) yielding the same $\delta n/n$ of TB96₂; (b) TB96₂ with the “standard” $D_0 = 0.27$, and the “renormalized” $D_0 = 0.24$ (strict₂) yielding the same $\delta n/n$ of TB96₁; (c) TB96₂ with its high- and low-density counterparts; (d) TB96₂ with its high- and low-velocity-dispersion counterparts (hot₂ and cold₂, respectively). The analogous group sample TB96NW₂, where both links (normalized as for TB96₂) were scaled with the recipe of NW87, is also shown. Errorbars (omitted for clarity) are always similar to those in Fig.3. Note how ξ_{GG} is only moderately sensitive to variations of D_L , while is almost independent from V_L ; it is particularly sensitive to the “parameter” m_{lim} (in fact, any intrinsic difference between the galaxy data sets PPS1 and PPS2).



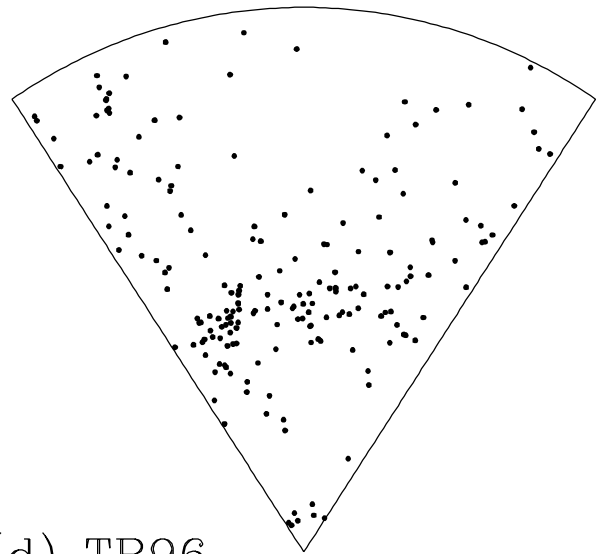
(a) PPS1



(b) PPS2



(c) TB96₁



(d) TB96₂

